Biochemical Pharmacology, Vol. 57, pp. 1283–1295, 1999.

ISSN 0006-2952/99/$–see front matter
PII S0006-2952(99)00046-5

Selective Toxicity of the Tricyclic Thiophene NSC 652287 in Renal Carcinoma Cell Lines

DIFFERENTIAL ACCUMULATION AND METABOLISM

Maria I. Rivera,† Sherman F. Stinson,* David T. Vistica,* Jean L. Jorden,‡ Susan Kenney* and Edward A. Sausville**

*Laboratory of Drug Discovery Research and Development, Developmental Therapeutic Program, Division of Cancer Treatment and Diagnosis, National Cancer Institute-Frederick Cancer Research and Development Center; and ‡SAIC-Frederick, National Cancer Institute-Frederick Cancer Research and Development Center, Frederick, MD 21702, U.S.A.

ABSTRACT. The tricyclic compound 2,5-bis(5-hydroxymethyl-2-thienyl)furan (NSC 652287) has shown a highly selective pattern of differential cytotoxic activity in the tumor cell lines comprising the National Cancer Institute (NCI) Anticancer Drug Screen. The mechanism underlying the selective cytotoxicity is unknown. We hypothesized that differential sensitivity to the compound observed in several renal tumor cell lines could be the result of selective accumulation or differential metabolism of this agent. We demonstrated here that the capacity of certain renal cell lines to accumulate and retain the compound, determined by accumulation of [^{14}C]NSC 652287-derived radioactivity and by flow cytometric determination of unlabeled compound, paralleled the sensitivity of the renal cell lines to growth inhibition by NSC 652287: A-498 > TK-10 ≫ ACHN ~ UO-31. The ability of the cell lines to metabolize [^{14}C]NSC 652287 to a reactive species capable of binding covalently to cellular macromolecules also directly correlated with sensitivity to the compound. Different patterns of metabolites were generated by relatively more drug-sensitive cell lines in comparison with drug-resistant cell lines. The metabolizing capacity for NSC 652287 was localized primarily to the cytosolic (S100) fraction. The rate of metabolism in the cytosolic fraction from the most sensitive renal cell line, A-498, was faster than that observed in the cytosolic fractions from the other, less sensitive cell lines. The data support the hypothesis that both selective cellular accumulation and the capacity to metabolize NSC 652287 to a reactive species by certain renal carcinoma cell types are the basis for the differential cytotoxicity of this compound class. BIOCHEM PHARMACOL **57**;11:1283–1295, 1999. © 1999 Elsevier Science Inc.

KEY WORDS. thiophene; renal carcinoma; antineoplastic agent; drug metabolism

The NCI§ Anticancer Drug Screen consists of a panel of 60 human tumor cell lines including leukemias and cancers of the skin, lung, colon, brain, ovary, kidney, prostate, and breast [1, 2]. The panel was established as a disease-oriented preclinical screening model to facilitate the discovery of novel drug leads with selective cytotoxicity toward solid tumors. The pattern of sensitivity to a new agent in the cell line screen provides a "fingerprint" that can be used as a tool to identify compounds of known or unknown mechanisms of action. The fingerprint of a given compound is analyzed by the computerized COMPARE algorithm [2–4], which describes the degree of similarity of the action of the new compound in comparison to that of standard agents. Structurally and/or mechanistically related compounds often have similar fingerprints. Tubulin-interactive antimitotics, topoisomerase inhibitors, antimetabolites, and alkylating agents, among others, have been identified by use of the COMPARE analysis [2–5, and references cited therein]. Current efforts are directed toward the quantitation of potential molecular targets for drug action in the tumor cell lines. These targets include oncogenes, tumor suppressor genes, drug resistance-mediating transporters, cell cycle proteins, apoptotic pathways, DNA repair enzymes, components of the cytoarchitecture, and drug metabolizing enzymes, among others [5]. The hypothesis is that the pattern of expression of a molecular target may be related to the pattern of cell susceptibility to agents directed at the target. Using this approach, substrates for the mdr-1/P-glycoprotein drug resistance transporter [6] and agents that target the epidermal growth factor receptor and c-erbB2 signaling pathways [7, 8] have been identified. It is expected that the molecular characterization of the cell lines will also help define molecular mechanisms not previously considered as drug targets.

† Corresponding author: Dr. Maria I. Rivera, Laboratory of Drug Discovery Research and Development, NCI-FCRDC, Bldg. 560, 32–60, Frederick, MD 21701-1201. Tel. (301) 846-5132; FAX (301) 846-6157.

§ *Abbreviations:* CYP450, cytochrome P450; GI_{50}, drug concentration that produces a 50% inhibition of cell growth; LC_{50}, drug concentration required to decrease the initial number of cells by 50%; NCI, National Cancer Institute; and XTT, 2,3-bis[2-methoxy-4-nitro-5-sulfophenyl]-5-[(phenylamino)-carbonyl]-2*H*-tetrazolium hydroxide.

Received 2 July 1998; accepted 30 October 1998.

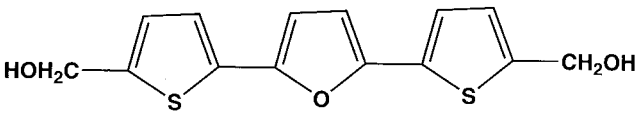

FIG. 1. Structure of NSC 652287, 2,5-bis(5-hydroxymethyl-2-thienyl)furan.

Thiophenes are sulphur-containing compounds widely distributed among plants of the family Asteraceae (Compositae) including many species with known medicinal uses [9]. Several naturally occurring and synthetic dithiophenes and terthiophenes have been shown to posses insecticidal, bactericidal, antifungal, and antiviral (including antiretroviral) activity [9–11]. Other thiophene-containing compounds have therapeutic applications, such as tienilic acid, a diuretic and uricosuric drug [12, 13], ZD 1694 (Tomudex), a thymidylate synthase inhibitor with activity against colorectal tumors [14, 15], and suprofen and tenoxicam, both non-steroidal anti-inflammatory agents [16, 17].

A series of naturally occurring and synthetic compounds containing one or more thiophene moieties have been tested in the NCI Anticancer Drug Screen and have demonstrated differential antiproliferative activity. Thiophene derivatives as a class exhibit very similar patterns of differential sensitivity, the molecular basis for which is not clear. The compound 2,5-bis(5-hydroxymethyl-2-thienyl) furan (NSC 652287, Fig. 1), is the most potent thiophene derivative and has been selected as the lead compound for mechanistic studies. This compound has notable activity against renal carcinoma cell lines, and this is of particular interest since there are few therapeutic options with reliable activity against metastatic renal cell carcinomas. The antitumor activity observed *in vitro* was retained *in vivo* using xenografts of the A-498 renal cell carcinoma in nude mice. The COMPARE algorithm analysis shows no similarity of the pattern of activity to the 170 standard antitumor agents in the NCI database. This unique pattern suggests that aspects of the action of the compound utilize a novel cell-type related mechanism for causing cytotoxicity. The present study was undertaken to determine factors responsible for the selective antiproliferative and cytotoxic activity of NSC 652287 in several renal carcinoma cell lines. Our findings suggest that both differential cellular accumulation and metabolism are determinants of the unique cytotoxicity of NSC 652287 in the renal cell lines studied.

MATERIALS AND METHODS

Materials

Cell culture reagents were purchased from Quality Biological, Inc. except for fetal bovine serum, which was purchased from HyClone Lab., Inc. NSC 652287 (purity > 99% as determined by LC-MS) was obtained from the repository of the NCI-Frederick Cancer Research and Development Center and originally was submitted to NCI by Dr. Michael Cava, University of Alabama. [^{14}C]NSC 652287 (19 mCi/mmol) was synthesized at the Research Triangle Institute. The synthesis of [^{14}C]NSC 652287 was accomplished by treatment of 2,5-bis(2-thienyl)furan with *n*-butyllithium and tetramethylenediamine in diethyl ether to generate the bis(5-lithiothienyl) derivative. Reaction of this dilithium salt with *N*-methyl([^{14}C]form)anilide gave the corresponding bis([^{14}C]carboxaldehyde), which was reduced directly by the addition of potassium triethylborohydrate to yield radiolabeled 2,5-bis(5-hydroxy [^{14}C]methyl-2-thienyl)furan (NSC 652287). Purification was accomplished by a combination of sequential chromatography on silica gel, dilution with unlabeled NSC 652287, and recrystallization. The final product was 99% radiochemically pure (as determined by TLC), with a ^{1}H-NMR spectrum identical to that of a standard sample of NSC 652287. For all experiments NSC 652287 was dissolved in DMSO and prepared as a 1000x stock. HPLC-grade acetonitrile was purchased from Baker. All other reagents were of the highest grade commercially available.

Cell Lines

The human renal tumor cell lines were obtained from the repository of NCI-FCRDC. The identities, sources, derivation, and morphological and immunocytochemical characteristics of the cell lines have been published previously [18–20]. Cells were grown in an atmosphere of 5% CO_2/95% air in RPMI-1640 medium supplemented with 10% fetal bovine serum, 100 U/mL penicillin, 100 μg/mL streptomycin, and 2 mM L-glutamine.

Drug Sensitivity Studies

Initial screening studies were conducted as described [21] using the sulforhodamine B protein assay. Examination to assess susceptibility of cells to a wider concentration range of NSC 652287 was done using the XTT assay as described by Scudiero *et al.* [22]. Cells were inoculated into 96-well flat-bottom plates at a density of 1500 cells per well and incubated for 24 hr at 37° in a humidified 5% CO_2/95% air atmosphere. Serial concentrations of NSC 652287 in DMSO were added to the wells, and sensitivity was determined 48 hr after the addition of the compound. Assessment of the *in vivo* activity of NSC 652287 in athymic mouse xenografts was conducted as described by Plowman *et al.* [23].

Cellular Uptake of [^{14}C]NSC 652287-Derived Radioactivity

Each cell line was grown in six-well plates until 60–70% confluent. Cells were incubated with 100 nM [^{14}C]NSC 652287 (19 mCi/mmol) for 0.5 to 72 hr. Medium was removed and plates were placed immediately on ice. Cell monolayers were rinsed rapidly three times with ice-cold PBS (150 mM NaCl, 5.6 mM Na_2HPO_4, 1.06 mM KH_2PO_4), pH 7.4, and solubilized at room temperature by incubation for 16 hr with 1 mL 0.2 N NaOH. The amount of [^{14}C]NSC 652287-derived radioactivity that had accu-

mulated intracellularly was quantitated by liquid scintillation spectrometry. Glacial acetic acid (2.75 mL/L) was added to the liquid scintillation fluid to prevent chemiluminescence in the alkaline solution. The results were expressed as picomoles per milligram of protein. Protein content was determined by the Coomassie Blue assay (Pierce) using BSA as standard.

Rate of Disappearance of NSC 652287 from the Cell Medium and Pattern of Metabolites Generated

Cells were grown in six-well plates until 60–70% confluent. NSC 652287 was added to a final concentration of 0.1 or 1 μM. Aliquots of the cell medium were removed at 0–48 hr and analyzed for levels of NSC 652287 and for presence of metabolites using HPLC with concurrent fluorescence and ultraviolet detection. At each time point, the cell monolayer was solubilized in 1 mL 0.2 N NaOH, and protein content was determined by the Coomassie Blue assay. In preliminary studies we observed that the soluble metabolites were found in the medium rather than intracellularly. Subsequently, we analyzed aliquots from the cell medium for the presence of metabolites generated by the cell lines. Half-lives ($T_{1/2}$) of drug disappearance were determined by nonlinear regression analysis of concentration *vs* time data using the geometric means of the compound concentrations (normalized for total protein content of the incubation wells).

Fluorescence excitation and emission spectra in the range 190–600 nm were obtained during chromatography (see below) with a HP 1046A programmable fluorescence detector. The detector was equipped with a xenon-arc flash-lamp (flash frequency 55 Hz), a 2 × 2 mm excitation slit (25 nm bandwidth), 4 × 4 mm emission slits (50 nm bandwidth), and a 5 μL flow cell. A 370-nm cutoff filter was inserted between the flow cell and the emission slit. Uncorrected spectra were measured by stopping the eluent flow, scanning at 6 nm/sec. The excitation spectrum was characterized by a maximum wavelength at 360 nm. Maximum emission was obtained at 420 nm.

The HPLC analysis was performed using a Hewlett Packard 1050 Series Module (pump, autosampler, and multiple wavelength detector) and a Hewlett Packard 1046A fluorescence detector. Fifty microliters of the sample was mixed with 150 μL acetonitrile to precipitate proteins. After centrifugation at 15,000 *g* (10 min), 150 μL of the supernatant was mixed with 225 μL of ammonium formate buffer, pH 4.0. The sample was vortexed, and 325 μL of the supernatant was injected into a 5-μm reverse-phase C_{18} analytical column (4.6 × 150 mm, YMC J′ Sphere-ODS-H80). Chromatography was effected with an isocratic eluent at a flow rate of 1 mL/min using a mobile phase consisting of acetonitrile:50 mM ammonium formate buffer, pH 4.0 (30:70, v/v) Fluorescence detection was performed using excitation and emission wavelengths of 360 and 414 nm, respectively. Concurrent ultraviolet detection was also performed at wavelengths of 200 and 365 nm to verify the specificity of the fluorescence detection, and to increase the probability of detection of metabolites whose fluorescence properties may have been altered. Under these conditions NSC 652287 has a retention time of 21 min. Hewlett Packard Chemstation software (v. 4.01) was used for data control and analysis. Calibration standards were prepared by sequential dilution of a 1 mM DMSO stock solution of the compound with cell culture medium or buffer containing the appropriate cell fraction inactivated by heating. The concentration of calibration standards was selected to cover the range of concentrations to be encountered in the specific study. Calibration curves were constructed by plotting the peak area against the theoretical concentration of the standard. The slope and y-intercept of the line of best fit was determined by linear least squares regression analysis.

In the experiments where we used ^{14}C-labeled NSC 652287, fractions of 0.25 to 2 min were collected following injection into the HPLC. Scintillation fluid was added to the samples (14 mL), and radioactivity was determined by liquid scintillation spectrometry.

Cellular Accumulation and Retention (Flow Cytometric Method)

Cells were grown in 162-cm^2 flasks until 60–70% confluent. The intracellular accumulation of 0–50 μM NSC 652287 was measured following a 30-min incubation. Medium was removed, and the cell monolayer was rinsed twice with ice-cold PBS. All steps were carried out at 4° to minimize efflux of the drug. Cells were released from the flasks by incubation for 5 min with 3 mL of cold trypsin (0.05%)-EDTA (0.1%). Seven milliliters of ice-cold PBS was added, and cells were sedimented by centrifugation at 300 *g* for 2 min. The sedimented cells were resuspended in 300 μL 1% paraformaldehyde in PBS and kept on ice in the dark. Aliquots containing 1 × 10^6 cells were used for analysis by flow cytometry.

In the retention experiments, cells were exposed to 10 μM NSC 652287 for 1 hr. Medium was removed and cells were rinsed twice with ice-cold PBS. Drug-free medium was added and incubation continued for 0–120 min. At the end of each period of time, the medium was removed and cells were rinsed twice with ice-cold PBS. Subsequent steps were done as described above for the drug accumulation experiments.

The fluorescence intensity retained within the cells and attributable to NSC 652287 was measured on a Coulter EPICS753 flow cytometer using a Coherent INNOVA 90 laser run at 30 mW in UV mode (Coulter Corporation). As mentioned in the previous section, NSC 652287 has maximum excitation and emission fluorescence at 360 and 420 nm, respectively, and these wavelengths were used for the analysis by flow cytometry. Ten thousand events were collected per sample. The results are expressed as either mean channel fluorescence (accumulation studies) or percentage of NSC 652287 retained (retention studies). Values were corrected for the endogenous fluorescence of the cells.

Covalent Binding to Cellular Proteins

Cells were grown in 75-cm^2 tissue culture flasks until 60–70% confluent. [^{14}C]NSC 652287 (19 mCi/mmol) was added to a final concentration of 0.25 to 1 μM. Following a 4- to 96-hr incubation, medium was removed and cells were rinsed twice with ice-cold PBS, pH 7.4. Cells were scraped off the plates, disrupted by sonication, and protein was precipitated with 10% trichloroacetic acid (final concentration). The protein pellet was washed exhaustively with 60° methanol to remove non-covalently bound radioactivity. The precipitated protein was solubilized with 1 N NaOH (80° for 15 min), and covalent binding was determined by liquid scintillation spectrometry. Glacial acetic acid (2.75 mL/L) was added to the liquid scintillation fluid to prevent chemiluminescence in the alkaline solution. Values were expressed as picomoles per milligram of protein. The extent to which [^{14}C]NSC 652287 was metabolized by each cell line was determined as described in the previous section.

Metabolism of NSC 652287 by Subcellular Fractions

Cells were grown in 560-cm^2 plates (PGC Scientifics) until 70–80% confluent. Cells were scraped off the plates, rinsed twice with ice-cold PBS, and incubated on ice for 10 min in a hypotonic buffer containing 5 mM Tris-HCl, pH 7.4, 10 mM KCl, 1.5 mM $MgCl_2$, 1.5 mM $CaCl_2$, 10 μg/mL leupeptin, 10 μg/mL aprotinin, and 0.5 mM PMSF. Cells were disrupted in a Potter-Elvehjem homogenizer (clearance = 0.08 to 0.13 mm) at a speed of 1000 rpm, using 15–25 strokes depending on the cell line. After homogenization, 2 M sucrose was added to a final concentration of 0.25 M. The subcellular fractions were isolated by differential centrifugation [24]. Briefly, cell homogenates were centrifuged at 1000 *g* for 10 min to precipitate nuclei, unbroken cells, and cell debris. The pellet was resuspended in isotonic buffer and centrifuged as above. The supernatant was centrifuged at 10,000 *g*, 20 min, to obtain the crude mitochondrial fraction. The mitochondrial pellet was resuspended in buffer and recentrifuged at 10,000 *g*. The 10,000 *g* supernatant was further centrifuged at 100,000 *g*, 40 min, to obtain the cytosolic (supernatant) and microsomal fractions (pellet). The microsomal pellet was resuspended in buffer and recentrifuged at 100,000 *g*. To determine the metabolism of NSC 652287 by the subcellular fractions, incubation reactions were carried out in 50 mM potassium phosphate buffer (pH 7.4), 10 mM $MgCl_2$, 1 mg/mL protein, ± 2 mM NADPH and 10 μM NSC 652287 at 37° for 0–4 hr. NSC 652287 remaining intact was analyzed by HPLC as described above.

Statistical Analysis

All data are expressed as means ± SD or SEM. Mean values were compared by ANOVA followed by *post hoc* Student–Newman–Keuls test to determine significance.

RESULTS

Screening Studies

Table 1 shows the concentrations of NSC 652287 producing 50% growth inhibition (GI_{50}) in the tumor cell lines of the NCI Anticancer Drug Screen after a 48-hr exposure to the compound. A number of cell lines showed a striking differential sensitivity to NSC 652287 when compared with the other cell lines in the panel, with GI_{50} values of 10–60 nM. The compound was found to decrease the initial number of cells by 50% (LC_{50}) at a concentration of 100 nM in the A-498 cell line, compared with ≥ 100 μM for the majority of the tumor cell lines (data not shown). NSC 652287 was evaluated against A-498 tumor cell xenografts grown subcutaneously in nude mice (Table 2). When NSC 652287 was administered twice a day (i.v. injections 7 hr apart) on an intermittent schedule (every 4 days for 12 days), all three doses resulted in complete tumor regression in 100% of the treated mice by the end of the third treatment period. The tumors did not regrow during the remaining 40 days of the study, and no gross evidence of toxicity was observed. Studies with xenografts derived from other sensitive cell lines including the renal CAKI-1, melanoma UACC-257, ovarian OVCAR-5, and colon HCC-2998, showed moderate or minimal *in vivo* activity [25]. In a separate series of experiments, *in vitro* time-course evaluation studies demonstrated that periods of exposure of the A-498 sensitive cell line to the compound as short as 0.75 hr were as effective in producing growth inhibition or cytotoxicity as exposure for up to 6 days (E. Sausville *et al.*, unpublished results). The ovarian OVCAR-5 and renal CAKI-1 cell lines were also relatively sensitive but required longer exposures and/or higher concentrations.

Response of Renal Cell Lines to NSC 652287

More detailed analysis of cytotoxicity was completed in a series of renal carcinoma cell lines. The A-498 and TK-10 cell lines were particularly sensitive to NSC 652287-induced cytotoxicity compared with ACHN and UO-31 cell lines (Fig. 2). The IC_{50} values were 2 nM, 20 nM, 13 μM, and 37 μM, respectively. The sensitivity obtained with this assay was in accord with that observed in the NCI Anticancer Drug Screen, and suggested that the renal subpanel of cell lines could be utilized to understand the basis for the selective cytotoxicity of NSC 652287.

Cellular Accumulation of [^{14}C]NSC 652287-Derived Radioactivity

Cells were exposed to 100 nM [^{14}C]NSC 652287 for 0.5 to 72 hr. This concentration of NSC 652287 was selected because it produced a marked difference in cytotoxicity between the sensitive and relatively resistant cell lines used in these studies (Fig. 2). The extent of accumulation of radioactivity in the most sensitive cell line, A-498, was 3–4 times greater than that of the cell line with intermediate sensitivity, TK-10 (Fig. 3). Both relatively resistant cell

TABLE 1. Growth inhibition by NSC 652287 in the NCI anticancer drug screen

Cell line	GI_{50} (μM)	Cell line	GI_{50} (μM)
Leukemia/lymphoma		Melanoma	
RPMI-8226	5.45 ± 2.97	MALME-3M	67.3 ± 22.4
SR	3.95 ± 0.70	M19-MEL	59.9
HL-60 (TB)	3.17 ± 0.47	SK-MEL-28	53.1 ± 16.6
MOLT-4	2.57 ± 0.93	M14	35.6 ± 10
CCRF-CEM	2.21 ± 0.83	SK-MEL-2	27.2 ± 1.2
K-562	1.03 ± 0.76	LOXIMVI	25.1 ± 4.5
		SK-MEL-5	24.0 ± 4.1
Non-small cell lung carcinoma		UACC-257	0.02 ± 0
HOP-92	36.9 ± 16.8	UACC-62	0.02 ± 0
EKBX	27.5 ± 3.1	Ovarian	
NCI-H522	24.6 ± 3.5	OVCAR-8	12.6 ± 1.9
NCI-H23	20.1 ± 6.4	SK-OV-3	12.4 ± 11.6
NCI-H322M	12.0 ± 5.49	OVCAR-4	0.17 ± 0.08
A549/ATCC	5.31 ± 2.39	OVCAR-3	0.14 ± 0.06
HOP-18	0.34	IGRO1	0.05 ± 0.01
HOP-62	0.33	OVCAR-5	0.03 ± 0.02
NCI-H226	0.07 ± 0.04		
NCI-H460	0.04 ± 0.01	Renal	
LXFL-529	0.02	UO-31	40.8 ± 10.4
		ACHN	27.8 ± 20.3
Small cell lung carcinoma		SN12C	6.24 ± 2.55
DMS 114	13.4	786-0	4.01 ± 1.02
DMS 273	0.73	RXF-393	0.79 ± 0.33
		TK-10	0.03 ± 0.01
Colon		A498	0.02 ± 0.01
KM-12	21.7 ± 5.7	CAKI-1	0.01 ± 0.00
HCT-15	0.77 ± 3.61		
DLD-1	5.21	Prostate	
HCC-2998	2.27 ± 1.53	PC-3	53.5 ± 18.0
HT29	0.98 ± 0.20	DU-145	7.21 ± 2.97
COLO 205	0.45 ± 0.13		
SW-620	0.25 ± 0.04	Breast	
HCT-116	0.11 ± 0.07	MDA-MB-231/ATCC	36.7 ± 16.7
KM20L2	0.01	HS 578T	25.0 ± 1.2
		MCF7/ADR-RES	20.0 ± 5.6
CNS		MDA-N	6.66 ± 3.03
SF-268	62.3 ± 18.3	MDA-MB-435	4.79 ± 1
SNB-19	49.6 ± 23.4	BT-549	3.58
SNB-75	41.0 ± 18.6	T-47D	0.43 ± 0.29
SF-539	35.1 ± 19.6	MCF7	0.07 ± 0.04
SF-295	10.3 ± 4.2		
U251	0.20 ± 0.10		
XF 498	0.06		

GI_{50} is the concentration that inhibited growth of the indicated cell line by 50% in a 48-hr continuous exposure to drug. Values are the means ± SEM, 3–5 separate experiments. Values with no SEM have N = 1 or 2.

lines, ACHN and UO-31, did not accumulate significant amounts of radioactivity for up to 96 hr. Therefore, the extent of accumulation of [^{14}C]NSC 652287-derived radioactivity paralleled the sensitivity of the cell lines to the compound.

Rate of Disappearance of NSC 652287 from the Cell Medium

The negligible amounts of accumulated radioactivity in the resistant cells could result from the lack of uptake of [^{14}C]NSC 652287 or from the ability of these cells to export the compound. To determine whether the resistant cell lines were able to take up NSC 652287, we measured the rate of disappearance of the compound from the culture medium. Figure 4 illustrates the results obtained at (A) 0.1 μM and (B) 1 μM NSC 652287. The rate of disappearance was more rapid in the two most sensitive cell lines ($T_{1/2}$ of 2.18 ± 0.01 and 3.0 ± 0.00 hr at 0.1 μM, and 4.42 ± 0.39 and 7.8 ± 0.9 hr at 1 μM for A-498 and TK-10, respectively). The rate of disappearance of NSC 652287 from the medium of the resistant cell lines was considerably slower ($T_{1/2}$ of 16.4 ± 4.1 and 145 ± 76 hr at 0.1 μM, and 38 ± 7.2 and 98 ± 34 hr at 1 μM for ACHN and UO-31, respectively). Thus, the rate of disappearance of NSC 652287 from the cell medium directly correlated with the sensitivity of the renal cell lines to the compound. It is

TABLE 2. *In vivo* activity of NSC 652287; advanced stage A-498 renal carcinoma athymic mouse xenografts

Dose (mg/kg) IV q 7 hr × 2*	No. of mice	Drug death	Tumor free	%T/C (day)†	Median day to 2 doublings‡
0	8	0	0	—	9.7
44.5	8	0	8	−100 (27)	UE§
66.7	8	0	8	−100 (24)	UE
100	8	0	8	−100 (24)	UE

*Schedule was started at day 18 after implant of the tumor cells. Three treatments were administered. The start of tumor regression was observed before beginning the second treatment day.

†T/C = Change in tumor weight for the treated group/change in tumor weight for the control group. Number in parentheses indicates day at which the optimum value was obtained. %T/C values < -50 are interpreted as tumor regression.

‡Median of the times (days) required for the tumor weights to increase by 2 doublings. Tumor-free survivors are excluded from the calculations.

§Unevaluable.

noteworthy that parental compound completely disappeared from the cell medium in the resistant ACHN cell line and decreased 40–50% in the resistant UO-31 cell line after incubation for 48 hr. At this time point, the intracellular accumulation of 100 nM [^{14}C]NSC 652287-derived radioactivity was still negligible (Fig. 3).

Cellular Uptake and Efflux (Flow Cytometry Studies)

Taking advantage of the fluorescent properties of NSC 652287, we studied in greater detail the ability of the renal cell lines to accumulate and retain the compound. In agreement with the study in which we measured the time-dependent accumulation of [^{14}C]NSC 652287-derived radioactivity (Fig. 3), the A-498 cells accumulated the compound to concentrations that were significantly higher than in the other cell lines (Fig. 5). This differential accumulation of the compound was concentration-dependent. At the 100 nM concentration (Fig. 5 insert), the mean channel fluorescence value in the A-498 cell line was 3-fold higher than in the TK-10 cell line, whereas only background fluorescence was detected in both resistant cell lines (ACHN and UO-31). The resistant cell lines required concentrations higher than 1 μM to substantially accumulate NSC 652287. At this concentration, the mean channel fluorescence value in the resistant cell lines was 20-fold lower than in the sensitive A-498 cell line. The difference in the mean channel fluorescence was less than 2-fold for all cell lines compared with A-498 cells at the highest concentration used (50 μM). The curve for the A-498 and TK-10 cell lines was biphasic. The slope of the line decreased at concentrations ≥ 1 μM.

The results of the efflux experiments in cells exposed to 10 μM NSC 652287 for 60 min are shown in Fig. 6. The A-498 cells retained more than 80% of the compound for up to 2 hr compared with 50% in the TK-10 cell line. In contrast, the mean channel fluorescence in both resistant cell lines decreased to background levels within 10 min after the removal of NSC 652287 from the cell medium.

Covalent Binding of [^{14}C]NSC 652287 to Cellular Proteins

In order to test the possibility that the differential accumulation of NSC 652287 reflects a difference in the ability of the sensitive cell lines to generate a reactive species capable

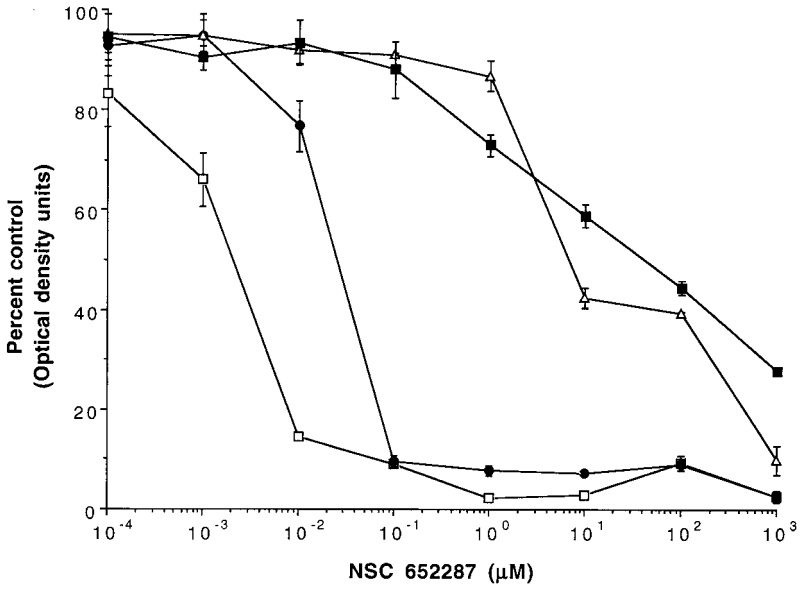

FIG. 2. Response of renal cells to NSC 652287 in a 48-hr XTT assay. Data are means ± SD (N = 3). Key: □, A-498; ●, TK-10; △, ACHN; ■, UO-31.

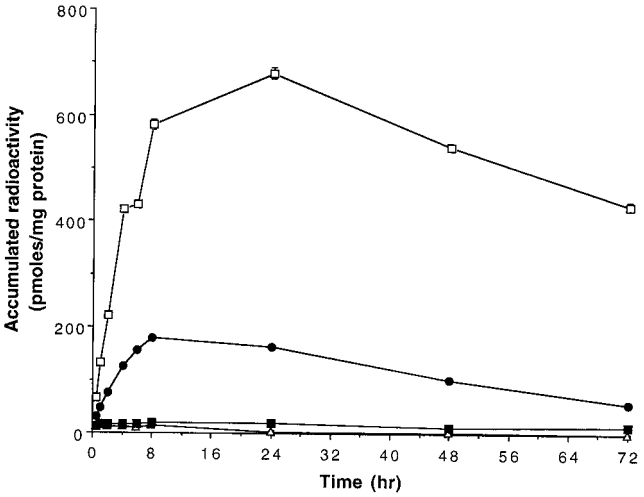

FIG. 3. Accumulation of [^{14}C]NSC 652287-derived radioactivity in renal carcinoma cell lines. Cells were exposed to 100 nM [^{14}C]NSC 652287 (19 mCi/mmol) for the specific times indicated in the figure. The cell monolayer was solubilized in 0.2 N NaOH and intracellular radioactivity was determined by liquid scintillation spectrometry. Data are means ± SD (N = 6). Key: □, A-498; ●, TK-10; △, ACHN; ■, UO-31.

of binding to cellular macromolecules, cells were incubated with several concentrations of [^{14}C]NSC 652287 for a period of 4 hr, and radioactivity covalently bound to cellular proteins was measured (Fig. 7). There was a concentration-dependent increase in label apparently bound covalently to proteins in the most sensitive cell line, A-498, and in the cell line with intermediate sensitivity, TK-10. The levels of covalent binding to proteins in the A-498 renal cell line were markedly higher (4- to 8-fold) than those in the TK-10 renal cell line. Both relatively resistant cell lines, ACHN and UO-31, had minor levels of covalent binding. Thus, the differential sensitivity to growth inhibition by the compound correlated directly with the ability of the cells to generate a reactive species capable of binding covalently to cellular macromolecules.

In Table 3 we compare the fraction of [^{14}C]NSC 652287 remaining in the medium with the levels of radioactivity covalently bound to proteins after incubation of the cell lines for several time intervals with 1 μM [^{14}C]NSC 652287. After a 4-hr incubation, the A-498 and TK-10 cell lines had a similar decrease in the medium concentration of compound (about 20%) but there was a 4-fold difference in the levels of covalent binding to cellular proteins. At the same time point, there was a 10% decrease in the concentration of [^{14}C]NSC 652287 in both ACHN and UO-31 resistant cell lines, which may explain the lower levels of covalent binding. Measurement of the levels of covalent binding to proteins at time points where little [^{14}C]NSC 652287 remained in the medium did show an increase in the levels of covalently bound radioactivity in the relatively resistant cell lines, which were maximum at 24 hr. However, these levels were substantially lower than those found in both the most sensitive A-498 cell line and the cell line with intermediate sensitivity, TK-10. For instance, at time points where the decrease in the concentration of [^{14}C]NSC 652287 was about 70%, the levels of covalent binding compared with those found in A-498 cells were 4-, 400-, and 200-fold less in TK-10, ACHN, and UO-31 cell lines, respectively.

Incubation of A-498 renal cell carcinoma with antioxidants such as catalase (100 U/mL), superoxide dismutase (100 μg/mL), and tempol (1 mM), or the iron chelator deferoxamine (500 μM, 2-hr preincubation), afforded no protection against the toxic effects of NSC 652287 (M. I. Rivera and J. Mitchell, unpublished results). In addition, there was no difference in cytotoxicity in cells incubated with NSC 652287 under aerobic *vs* hypoxic conditions. The evidence argues against formation of reactive oxygen species as the mechanism leading to NSC 652287-induced cytotoxicity in A-498 cells.

Different Pattern of NSC 652287 Metabolites Generated in the Sensitive and Resistant Renal Carcinoma Cell Lines

The formation of metabolites derived from [^{14}C]NSC 652287 was analyzed after a 4-, 24-, 48-, and 96-hr incubation. Figure 8 shows the profile of radioactive metabolites generated following incubation with 1 μM [^{14}C]NSC 652287 at a time point when a similar concentration of compound remained in the medium (20–30% of the initial concentration). Within each cell line, the same profile of metabolites was obtained at the time intervals analyzed although the amount of each metabolite varied with time (data not shown). All cell lines produced two metabolites with retention times of 7 and 12 min. The radioactivity in the 12-min peak was minor and accounted for less than 5% of the total radioactivity injected into the HPLC for all cell lines and at all time points. The amount formed of the metabolite eluting at 7 min was significantly greater in the resistant cell lines (35 and 30% in ACHN and UO-31, respectively, *vs* 10% in both A-498 and TK-10). Two additional, more polar metabolites were detected in the sensitive cell lines. Both A-498 and TK-10 cells produced the metabolite eluting at 5 min. This was the major metabolite generated in the A-498 cell line (15%). The metabolite eluting at 3.75 min was detected only in the TK-10 cell line and was the major one accounting for 25% of the total radioactivity injected into the HPLC.

Metabolism of NSC 652287 by A-498 Subcellular Fractions

Cellular components of the A-498 cell line were separated using differential centrifugation to determine the subcellular fraction(s) responsible for the metabolism of NSC 652287. Cell homogenates metabolized 80% of the compound by 4 hr, and the metabolic capacity was lost upon incubation of the homogenates at 95° (Table 4). The metabolism of NSC 652287 was concentrated primarily in the cytosolic fraction (S100), where the compound was

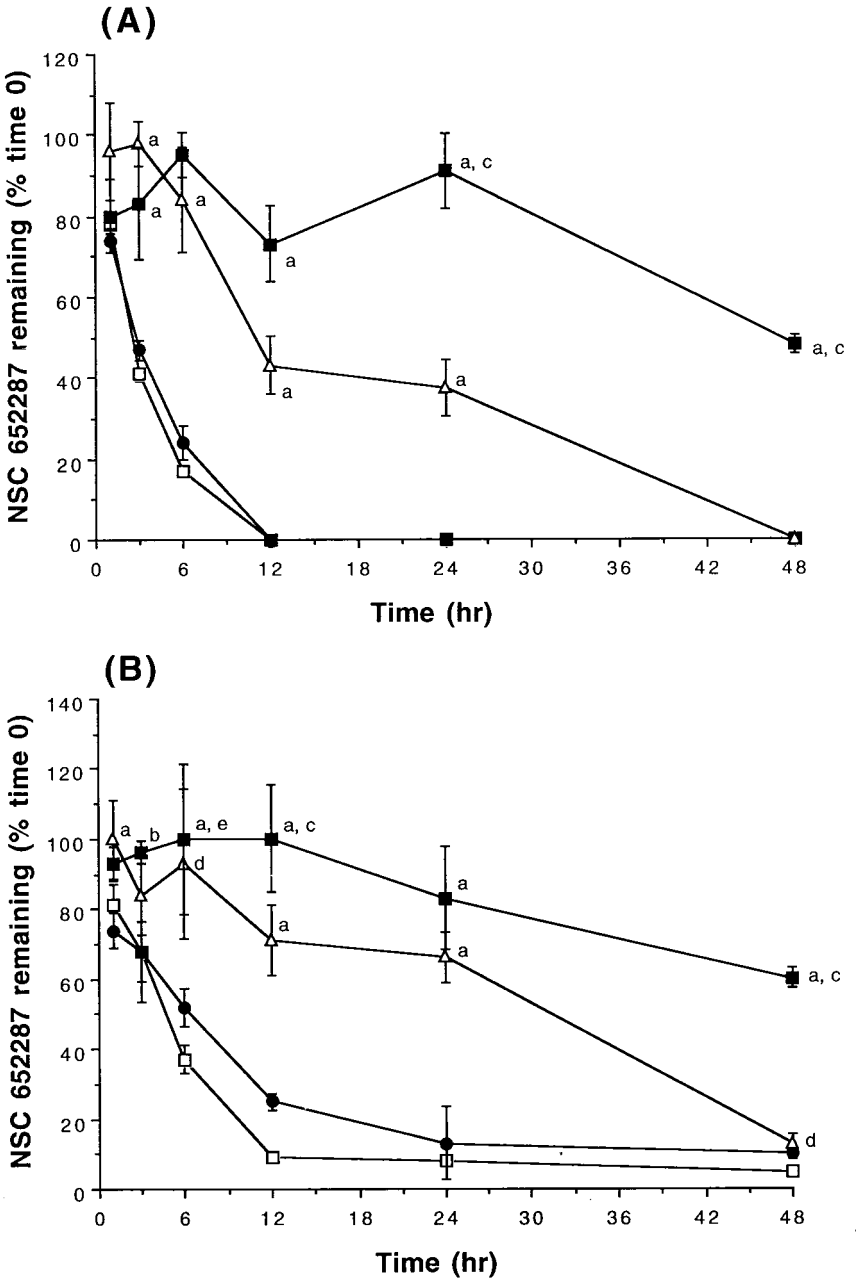

FIG. 4. Disappearance of NSC 652287 from the cell medium. Cell lines were incubated with (A) 0.1 μM or (B) 1 μM NSC 652287. At selected time intervals, an aliquot of the medium was removed and analyzed for levels of compound using HPLC with concurrent fluorescence and ultraviolet detection as described in Materials and Methods. Data are means ± SD (N = 3). Significantly different from A-498 and TK-10 at $^{a}P < 0.01$ or $^{b}P < 0.05$, ^{c}ACHN at $P < 0.01$, ^{d}A-498 at $P < 0.01$, ^{e}TK-10 at $P < 0.01$. NSC 652287 was stable in culture medium for the entire duration of the experiment. Time 0 values (nmol NSC 652287/mg protein) for 0.1 and 1 μM cultures, respectively: A-498, 1.79 ± 0.07 & 18.2 ± 1.22; TK-10, 2.03 ± 0.13 & 19.5 ± 0.94; ACHN, 1.14 ± 0.07 & 12.5 ± 0.30; UO-31, 1.71 ± 0.03 & 17.1 ± 0.72. Key: □, A-498; ●, TK-10; △, ACHN; ■, UO-31.

metabolized almost completely by 2 hr. Some metabolic activity was also present in the nuclear (P1) and mitochondrial (P10) fractions. In these fractions, however, more than 50% of the drug still remained by 2 hr. The microsomal fraction (P100) showed minimal metabolic activity. The addition of NADPH to the incubation reaction resulted in a decrease in the extent of NSC 652287 metabolized by the cell homogenate and subcellular fractions. For instance, in the S100 fraction containing exogenous NADPH approximately 70% NSC 652287 remained unmetabolized by 2 hr. In contrast, nearly complete metabolism had occurred in the absence of exogenous NADPH at the same time point.

Metabolism of NSC 652287 by S100 Fractions from the Renal Carcinoma Cell Lines

The rate of metabolism of NSC 652287 by S100 fractions was cell line-dependent (Fig. 9). Consistent with the sensitivity to growth inhibition and cytotoxicity induced by NSC 652287, S100 fractions from A-498 cells showed a higher capacity to metabolize the compound. In this fraction, the concentration of NSC 652287 decreased to 30% by 1 hr, with complete disappearance by 2 hr. In contrast, 50–80% of NSC 652287 still remained intact by 2 hr in the incubations containing S100 fractions from the other cell lines.

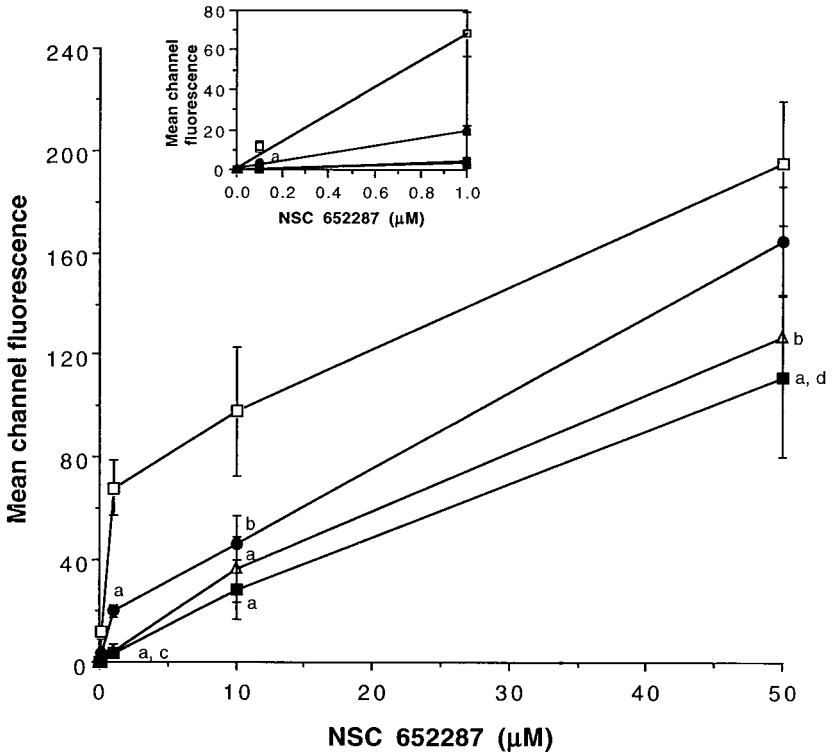

FIG. 5. Concentration curve for the accumulation of NSC 652287. Cell lines were incubated with 0.01, 0.1, 1, 10, and 50 μM NSC 652287 for 30 min. At the end of treatment, cells were fixed in 1% paraformaldehyde, and aliquots containing 1×10^6 cells were used for analysis by flow cytometry as described in Materials and Methods. Data represent the means ± SD of three separate experiments. Insert shows data points at ≤ 1 μM. Significantly different from A-498 cell line at $^aP < 0.01$ or $^bP < 0.05$; from TK-10 cell line at $^cP < 0.01$ or $^dP < 0.05$. Key: □, A-498; ●, TK-10; △, ACHN; ■, UO-31.

DISCUSSION

The experiments presented in this paper have led to the following conclusions. First, NSC 652287 caused selective growth inhibition in a variety of tumor cell lines from the NCI Anticancer Drug Screen, with notable activity in several renal carcinoma cell lines. The pattern of activity was distinct from that of the standard anticancer agents, suggesting a new mechanism for the anticancer activity. Second, the compound was particularly cytotoxic to the A-498 renal carcinoma cell line, and this activity was retained *in vivo* in the athymic nude mice xenograft model. Third, sensitive renal carcinoma cell lines had enhanced capacity to accumulate and retain NSC 652287 and to transform the compound to a form capable of binding

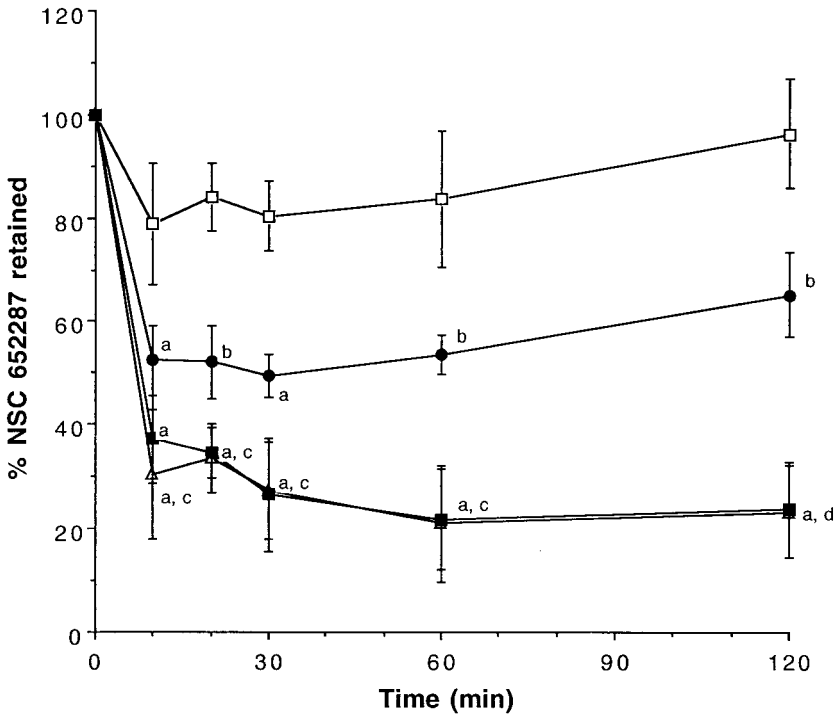

FIG. 6. Efflux of NSC 652287. Cell lines were incubated with 10 μM NSC 652287 for a period of 1 hr. Compound was removed and incubation continued for several times up to 2 hr. At the end of treatment, cells were fixed in 1% paraformaldehyde, and aliquots containing 1×10^6 cells were used for analysis by flow cytometry as described in Materials and Methods. Data represent the means ± SD of three separate experiments. Significantly different from A-498 cell line at $^aP < 0.01$ or $^bP < 0.05$; from TK-10 cell line at $^cP < 0.01$ or $^dP < 0.05$. Time 0 values (mean channel fluorescence): A-498, 144 ± 13; TK-10, 66 ± 18; ACHN, 39 ± 13; UO-31, 28 ± 8. Key: □, A-498; ●, TK-10; △, ACHN; ■, UO-31.

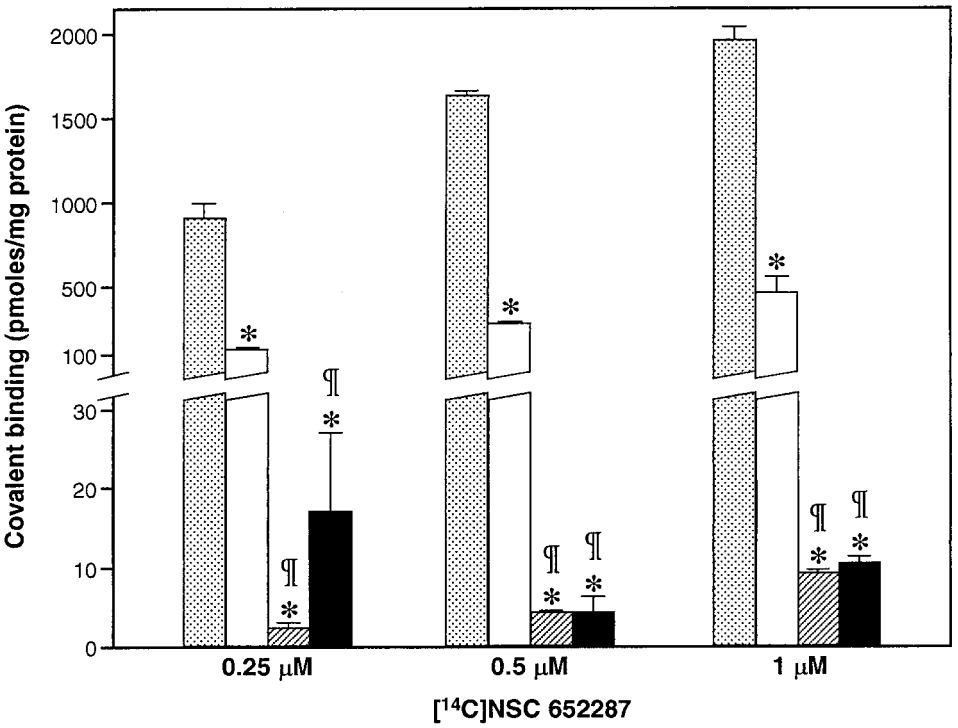

FIG. 7. Covalent binding of [^{14}C]NSC 652287 to proteins. The cell lines were incubated with NSC 652287 for 4 hr. Medium was removed and covalent binding was determined in the precipitated proteins as described in Materials and Methods. Data are means ± SEM (N = 3). Significantly different from *A-498 or ¶TK-10 at a given concentration ($P \leq 0.01$). The difference between concentrations for a given cell line was significant for A-498, TK-10, and ACHN ($P \leq 0.05$). Stippled bars, A-498; open bars, TK-10; hatched bars, ACHN; solid bars, UO-31.

covalently to cellular proteins. These results are consistent with the hypothesis that the capacity of the cells to metabolize NSC 652287 to a reactive species is crucial for eliciting cytotoxicity in the renal cell lines studied, and the presence of this metabolizing system(s) also may determine sensitivity in other tumor cell types.

Different factors may determine the intrinsic sensitivity or resistance of cells to the biological effect of an agent. These factors have been grouped into three major mechanisms for selective toxicity [26]. A biologically active agent can exert selectivity of effect either by differences in drug distribution in an organism, differences in biochemical properties of the target cells, or through interaction with a cytological feature that exists only in the susceptible cells. Often, two or more of these factors can function together to confer drug selectivity. In this investigation, we focused on whether accumulation and metabolism might be the basis for the selective toxicity of NSC 652287 in several renal cell lines from the NCI tumor cell line panel.

We considered first whether the renal carcinoma cell lines might differentially accumulate NSC 652287. We found a direct correlation between the accumulation of [^{14}C]NSC 652287-derived radioactivity and the sensitivity of the cell lines to the compound (Fig. 3). The lack of accumulation of radioactivity in the resistant cell lines (ACHN and UO-31) could be interpreted as lack of uptake of NSC 652287 in these cell lines. However, studies of the rate of disappearance of NSC 652287 from the medium demonstrated that, indeed, all four cell lines were able to take up the compound, and the rate of uptake directly correlated with the sensitivity to NSC 652287 (Fig. 4). The data were confirmed by flow cytometry experiments in

TABLE 3. Comparison of covalent binding to cellular proteins and % [^{14}C]NSC 652287 remaining in the cell medium

Cell line and incubation time	Covalent binding (pmol/mg protein)	% [^{14}C]NSC 652287 Remaining
A-498		
0 hr	29.7 ± 3.48	92.7 ± 2.08
4 hr	2705 ± 151	78.7 ± 2.08
24 hr	11732 ± 391	42.0 ± 6.24
48 hr	13157 ± 1046	35.3 ± 6.66
TK-10		
0 hr	17.5 ± 0.40	92.7 ± 1.15
4 hr	703 ± 3.10	73.3 ± 3.06
24 hr	3264 ± 246	27.3 ± 6.11
48 hr	4694 ± 429	11.3 ± 3.51
ACHN		
0 hr	3.18 ± 0.41	96.0 ± 5.29
4 hr	9.22 ± 0.76	88.0 ± 6.56
24 hr	31.2 ± 1.50	28.8 ± 17.6
48 hr	25.1 ± 1.79	10.6 ± 2.92
96 hr	12.5 ± 0.79	0
UO-31		
0 hr	4.69 ± 0.54	96.0 ± 5.29
4 hr	10.5 ± 1.45	92.7 ± 5.86
24 hr	96.9 ± 8.57	81.7 ± 1.53
48 hr	92.7 ± 1.83	61.7 ± 1.53
96 hr	62.0 ± 0.58	35.3 ± 7.51

Cell lines were incubated with 1 μM [^{14}C]NSC 652287 for the indicated times. Cell medium was removed and analyzed for levels of [^{14}C]NSC 652287 remaining as described in Materials and Methods. Protein was precipitated with 10% TCA, and the amount of covalent binding was determined after exhaustive washes with 60° methanol to remove non-covalently bound radioactivity. Metabolism of [^{14}C]NSC 652287 by A-498 cells reached a plateau by 24 hr as a consequence of extensive cell death as observed by light microscopy. Radiolabeled compound was found to be stable for up to 96 hr when incubated in medium under the same conditions as the cell lines. Values are means ± SD (N = 3).

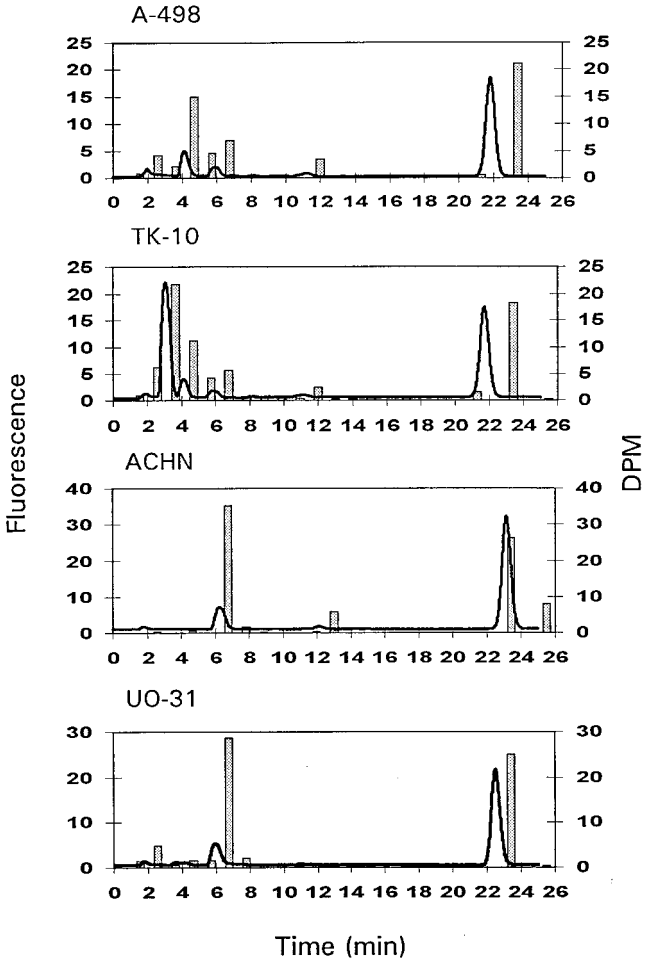

FIG. 8. Pattern of NSC 652287 metabolites generated in the sensitive and resistant renal tumor cell lines. Cells were exposed to 1 μM [^{14}C]NSC 652287 for selected time intervals, at the end of which an aliquot of the medium was removed and analyzed by HPLC and scintillation counting spectrometry as described in Materials and Methods. Profiles represent time points at which a similar concentration of thiophene remained in the medium (30%). Bars, radioactivity detection (dpm/fraction of 0.25 to 2 min); line, fluorescence detection (% Fluorescence × sec). Parameters are expressed as % time 0. The offset of the dpm bar from the chromatographic peak is due to the delay from the time the peak was detected by the fluorescence detector and when it actually reached the fraction collector, and the times, relative to this, over which the fractions were programmed to be collected.

which we utilized the fluorescent properties of NSC 652287 to analyze intracellular drug accumulation (Figs. 5 and 6). The sensitive cells retained a substantial fraction of thiophene-derived fluorescence, whereas rapid efflux of the compound occurred in the resistant cells. These results could argue in favor of an efflux mechanism present in the resistant cells, but they do not rule out the possibility that the resistant cell lines have a decreased capacity to metabolize NSC 652287. In addition, the resistant cell lines may generate non-toxic species that are released into the medium. The fact that the resistant cell lines accumulated negligible amounts of radioactivity (Fig. 3) at time points

TABLE 4. Metabolism of NSC 652287 by A-498 renal carcinoma cell line homogenate and subcellular fractions

Subcellular fraction	NSC 652287 remaining (% time 0)			
	− NADPH		+ NADPH	
	2 hr	4 hr	2 hr	4 hr
Control	100 ± 0.68	98 ± 8.54	90 ± 8.12	92 ± 7.88
Homogenate	39 ± 7.12	19 ± 2.41	66 ± 1.42	39 ± 0.11
Boiled homogenate	90 ± 0.41	81 ± 0.60	90 ± 1.56	89 ± 8.59
P1	56 ± 4.61	47 ± 0.70	77 ± 7.47	58 ± 3.66
P10	52 ± 5.77	33 ± 3.16	70 ± 1.52	48 ± 3.26
S10	26 ± 3.55	0.37 ± 0.14	73 ± 0.45	51 ± 4.26
P100	75 ± 1.46	76 ± 1.84	93 ± 0.44	92 ± 0.48
S100	1.3 ± 0.46	0	66 ± 2.51	27 ± 1.36

Incubation reactions were carried out in 50 mM potassium phosphate buffer (pH 7.4), 10 mM $MgCl_2$, ± NADPH, 1 mg/mL protein, and 10 μM NSC 652287 (10 nmol/mg protein) at 32° for 2–4 hr. Compound remaining intact was analyzed by HPLC with concurrent fluorescence and UV detection. Data represent the means ± SD (N = 3). Control contains all incubation components except protein.

when most of the compound has disappeared from the medium (Fig. 4) is consistent with this view. In contrast, NSC 652287 fluorescence remained at a constant level in the sensitive cell lines during the remaining 2-hr incubation period after the removal of the compound (Fig. 6), consistent with the view that sensitive cells generate a

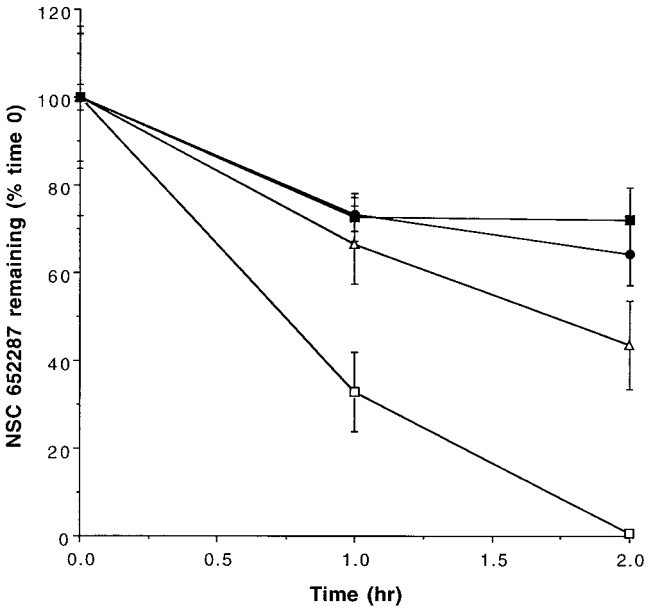

FIG. 9. Metabolism of NSC 652287 by S100 fractions from renal carcinoma cell lines. Incubation reactions were carried out in 50 mM potassium phosphate buffer (pH 7.4), 10 mM $MgCl_2$, 1 mg/mL S100 protein, and 10 μM NSC 652287 (10 nmol/mg protein) at 37° for 0–2 hr. Compound remaining intact was analyzed by HPLC with concurrent fluorescence and ultraviolet detection as described in Materials and Methods. Data are means ± SD (N = 3). Values for all cell lines were significantly different from those of A-498 ($P \leq 0.01$) at both 1 and 2 hr. Value for ACHN was significantly different from UO-31 at 2 hr ($P \leq 0.01$). Key: □, A-498; ●, TK-10; △, ACHN; ■, UO-31.

species which binds covalently to intracellular macromolecules.

To further investigate whether metabolism was important for the selective toxicity of the compound, we determined the ability of the cell lines to generate radioactivity covalently bound to cellular proteins following a 4-hr incubation with several concentrations of [^{14}C]NSC 652287. The formation of covalently bound label to proteins paralleled the sensitivity of the cell lines to NSC 652287 (Fig. 7). Since at 4 hr negligible accumulation/metabolism has occurred in the resistant cell lines, we measured the levels of covalent binding to proteins at later time points when little compound remained in the medium. At these time points, the levels of covalent binding in the resistant cell lines were still very low compared to those found in either A-498 or TK-10 cells (Table 3). Therefore, these findings support the hypothesis that the selective cytotoxicity results from the capacity of the cell lines to metabolize NSC 652287 to a reactive species that can bind covalently to cellular macromolecules. This process seems to occur rapidly in the sensitive cell lines. In contrast, in the resistant cell lines, the metabolism of NSC 652287 may not be as rapid and likely yields species with little capacity to bind to cellular components. In fact, the metabolism of the compound was faster in cytosolic fractions (S100) from the most sensitive cell line A-498 (Fig. 9). Therefore, the patterns of NSC 652287 accumulation and efflux appear to reflect differences in drug metabolism among the renal cell lines. The view of distinct metabolic pathways is further supported by the different pattern of metabolites detected by HPLC (Fig. 8). At time points where a similar amount of NSC 652287 has been metabolized, both sensitive cell lines have early eluting metabolites (more polar) as primary peaks, whereas a metabolite eluting later was primarily generated by the resistant cell lines.

The compound accumulation curve for the sensitive cell lines (Fig. 5) had two distinct phases, suggesting the involvement of a low capacity (saturable) component. This observation is intriguing in the context of our findings that sensitive cells can metabolize NSC 652287 to a species capable of covalent interaction with proteins. It raises the possibility that a saturable facilitated transport into susceptible cells may present large quantities of compound to a metabolizing system. Alternatively, NSC 652287 uptake may be driven by the metabolizing system itself, which may saturate.

CYP450 has been reported to play a central role in the metabolic activation of certain thiophene derivatives [27–29]. For instance, tienilic acid, a diuretic and uricosuric thiophene involved in rare cases of immunoallergic hepatitis, is oxidized mainly by CYP450 2C9 [30]. This reaction results in the formation of an electrophilic species capable of binding to liver proteins including P450 itself. Binding to CYP450 leads to suicide inactivation of the enzyme. However, our finding that metabolism of NSC 652287 is concentrated primarily in the cytosolic fraction argues strongly against a role for CYP450 in the metabolism of thiophene in the A-498 renal cell carcinoma. The reason for the decrease in the metabolic rate of thiophene when NADPH was added to the incubations is unknown but suggests inhibition of an oxidative step in the metabolism of the compound. Experiments presently are underway in our laboratory to purify the metabolizing system and characterize the nature of the reactive species.

The extent of covalent binding to macromolecular cell components paralleled sensitivity of the renal carcinoma cell lines to the compound. Although this may reflect the rate of bioactivation of the drug, it is possible that the mechanism of toxicity of NSC 652287 involves covalent binding to critical cellular components. The extensive covalent binding of reactive metabolites to proteins (or other cellular macromolecules) may cause major structural modifications that result in a loss of essential biochemical functions. We have obtained evidence that supports formation of DNA cross-links as a potential mechanism leading to growth inhibition and cell death [31].

In summary, we have used a subpanel of four renal carcinoma cell lines from the NCI Anticancer Drug Screen to identify factors responsible for the selective cytotoxicity and growth inhibition patterns of the tricyclic agent NSC 652287. Our data suggest that both cellular accumulation and the ability of the cell lines to metabolize the compound to a reactive species are major factors responsible for the differential antiproliferative activity. High levels of covalent binding to proteins were observed in the sensitive cell lines, and led to the hypothesis that covalent binding to essential cellular components is relevant to the antiproliferative mechanism of action of NSC 652287. Further investigations are warranted to elucidate the mechanism for the growth inhibitory and cytotoxic activity of this thiophene-containing compound.

This project has been funded in whole or in part with Federal funds from the National Cancer Institute, National Institutes of Health, under Contract No. N01-CO-56000. We gratefully acknowledge Dr. Nuri Neamati (Laboratory of Molecular Pharmacology, Division of Basic Sciences, National Cancer Institute) for his help with the preparation of the protocol for the flow cytometry studies. We appreciate the assistance of Louise R. Finch (SAIC, FCRDC) in performing the flow cytometric analysis. We also thank Tanya R. Prather, Jennifer A. Michael, and Shannon Berg (LDDRD, FCRDC) for their technical assistance with the XTT assays. Design of the synthetic scheme and synthesis of [^{14}C]NSC 652287 was accomplished by Dr. Jack A. Kepler and Dr. Kenneth S. Render of Research Institute (Research Triangle Park, NC) under NCI Contract N01-CM-47008. The content of this publication does not necessarily reflect the views or policies of the Department of Health and Human Services, nor does mention of trade names, commercial products, or organizations imply endorsement by the U.S. Government.

References

1. Boyd MR, The future of drug development. In: *Current Therapy in Oncology* (Ed. Niederhuber JE), pp. 11–22. BC Decker, Inc., Philadelphia, 1993.
2. Boyd MR and Paull K, Some practical considerations and

applications of the National Cancer Institute *in vitro* anticancer drug discovery screen. *Drug Dev Res* **34**: 91–109, 1995.
3. Paull KD, Shoemaker RH, Hodes L, Monks A, Scudiero DA, Rubinstein L, Plowman J and Boyd MR, Display and analysis of patterns of differential activity of drugs against human tumor cell lines: Development of mean graph and COMPARE algorithm. *J Natl Cancer Inst* **81**: 1088–1092, 1989.
4. Boyd MR, Paull KD and Rubinstein LR, Data display and analysis strategies for the NCI disease oriented *in vitro* antitumor drug screen. In: *Cytotoxic Anticancer Drugs: Models and Concepts for Drug Discovery and Development* (Eds. Valeriote FA, Korbit T and Baker L), pp. 11–34. Academic Publishers, Boston, 1992.
5. Weinstein JN, Myers TG, O'Connor PM, Friend SH, Fornace AJ Jr, Kohn KW, Fojo T, Bates SE, Rubinstein LV, Anderson NL, Buolamwini JK, van Osdol WW, Monks AP, Scudiero DA, Sausville EA, Zaharevitzm DW, Bunow B, Viswanadhan VN, Johnson GS, Wittes RE and Paull KD, An information-intensive approach to the molecular pharmacology of cancer. *Science* **275**, 343–349, 1997.
6. Alvarez M, Paull K, Monks A, Hose C, Lee J-S, Weinstein J, Grever MR, Bates S and Fojo T, Generation of a drug resistance profile by quantitation of mdr-1/P-glycoprotein expression in the cell lines of the National Cancer Institute Anticancer Drug Screen. *J Clin Invest* **95**: 2205–2214, 1995.
7. Bishop PC, Wosikowski K, Myres TG, Weinstein JN, Sausville E, Paull KD and Bates SE, Identification of compounds targeting the epidermal growth factor receptor signaling pathway using the NCI drug screen database. *Proc Am Assoc Cancer Res* **39**: 303, 1998.
8. Wosikowski K, Schuurhuis D, Johnson K, Paull KD, Myers TG, Weinstein JN and Bates SE, Identification of epidermal growth factor receptor and c-erbB2 pathway inhibitors by correlation with gene expression patterns. *J Natl Cancer Inst* **89**: 1505–1515, 1997.
9. Kagan J, Naturally ocurring di- and trithiophenes. *Prog Chem Nat Prod* **56**: 87–169, 1991.
10. Hudson JB, Graham EA, Miki N, Towers GHN, Hudson LL, Rossi R, Carpita A, and Neri D, Photoactive antiviral and cytotoxic activity of synthetic thiophenes and their acetylenic derivatives. *Chemosphere* **19**: 1329–1343, 1989.
11. Hudson JB, Harris L, Marles RJ and Arnason JT, The anti-HIV activities of photoactive terthiophenes. *Photochem Photobiol* **58**: 246–250, 1993.
12. Frohlich ED, Ticrynafen: A new thiazid-like but uricosuric antihypertensive diuretic. *N Engl J Med* **301:** 1378–1382, 1979.
13. Lemieux G, Kiss A, Vinay P and Gougoux A, Nature of the uricosuric effect of tienilic acid, a new diuretic. *Kidney Int* **12:** 104–114, 1977.
14. Jackman AL, Farrugia DC, Gibson W, Kimbell R, Harrap KR, Stephens TC, Azab M and Boyle FT, ZD1694 (Tomudex): A new thymidylate synthase inhibitor with activity in colorectal cancer. *Eur J Cancer* **31**: 1277–1282, 1995.
15. Rustum YM, Harstrick A, Cao S, Vanhoefer U, Yin M-B, Wilke H and Seeber S, Thymidylate synthase inhibitors in cancer therapy: Direct and indirect inhibitors. *J Clin Oncol* **15**: 389–400, 1997.
16. Abelson MB and Sloan J, Nonsteroidal anti-inflammatory drugs. Current ophthalmic therapy. *J Fla Med Assoc* **81**: 261–263, 1994.
17. Gentiletti AA, Tenoxicam, a new non-steroidal anti-inflammatory drug in the prolonged treatment of rheumatoid arthritis. *Eur J Rheumatol Inflamm* **9**: 91–94, 1987.
18. Alley MC, Scudiero DA, Monks A, Hursey ML, Czerwinski MJ, Fine DL, Abbot BJ, Mayo JG, Shoemaker RH and Boyd MR, Feasibility of drug screening with panels of human tumor cell lines using a microculture tetrazolium assay. *Cancer Res* **48**: 589–601, 1988.
19. Monks A, Scudiero D, Skehan P, Shoemaker R, Paull K, Vistica D, Hose C, Langley J, Cronise P, Vaigro-Wolff A, Gray-Goodrich M, Campbell H, Mayo J and Boyd MR, Feasibility of a high-flux anticancer drug screen using a diverse panel of cultured human tumor cell lines. *J Natl Cancer Inst* **83**: 757–766, 1991.
20. Stinson SF, Alley MC, Kopp WC, Fiebig H-H, Mullendore LA, Pittman AF, Kenney S, Keller J and Boyd MR, Morphological and immunocytochemical characteristics of human tumor cell lines for use in a disease-oriented anticancer-drug screen. *Anticancer Res* **12**: 1035–1054, 1992.
21. Skehan P, Storeng R, Scudiero D, Monks A, McMahon J, Vistica D, Warren JT, Bokesch H, Kenney S and Boyd MR, New colorimetric cytotoxicity assay for anticancer drug screening. *J Natl Cancer Inst* **82**: 1107–1112, 1990.
22. Scudiero DA, Shoemaker RH, Paull KD, Monks A, Tierney S, Nofziger TH, Currens MJ, Seniff D and Boyd MR, Evaluation of a soluble tetrazolium/formazan assay for cell growth and drug sensitivity in culture using human and other tumor cell lines. *Cancer Res* **48**: 4827–4833, 1988.
23. Plowman J, Dykes DJ, Hollingshead M, Simpson-Herren L and Alley MC, Human tumor xenograft models in NCI drug development. In: *Anticancer Drug Development Guide: Preclinical Screening, Clinical Trials and Approval*. (Ed. Teicher B), pp. 101–125. Humana Press, Totowa, 1997.
24. Graham J, Isolation of subcellular organelles and membranes. In: *Centrifugation, a Practical Approach* (Ed. Rickwood D), pp. 161–182. IRL Press, Oxford, 1984.
25. Carter CA, Waund WR, Plowman J and Alley MC, *In vivo* spectrum of antitumor activity of a thiophene derivative, NSC 652287D. *Proc Am Assoc Cancer Res* **37**: 393, 1996.
26. Albert A, *Selective Toxicity: The Physico-Chemical Basis of Therapy*. Chapman & Hall, New York, 1985.
27. Mansuy D, Valadon P, Erdelmeier I, Lopez-Garcia P, Amar C, Girault J-P and Dansette PM, Thiophene *S*-oxides as new reactive metabolites: Formation by cytochrome P450 dependent oxidation and reaction with nucleophiles. *J Am Chem Soc* **113**: 7825–7826, 1991.
28. Dansette PM, Thang DC, Elamri H and Mansuy D, Evidence for thiophene-*S*-oxide as a primary reactive metabolite of thiophene *in vivo*: Formation of a dihydrothiophene sulfoxide mercapturic acid. *Biochem Biophys Res Commun* **186**: 1626–1630, 1992.
29. Valadon P, Dansette PM, Girault J-P, Amar C and Mansuy D, Thiophene sulfoxides as reactive metabolites: Formation upon microsomal oxidation of a 3-aroylthiophene and fate in the presence of nucleophiles *in vitro* and *in vivo*. *Chem Res Toxicol* **9**: 1403–1413, 1996.
30. Lopez-Garcia MP, Dansette PM and Mansuy D, Thiophene derivatives as new mechanism-based inhibitors of P450: Inactivation of yeast-expressed human liver P450 2C9. *Biochemistry* **33**: 166–175, 1994.
31. Nieves-Neira W, Rivera MI, Hursey M, Sausville EA and Pommier Y, DNA damage induced by the thiophene NSC 652287 in renal cell lines of the National Cancer Institute (NCI) Anticancer Drug Screen. *Proc Am Assoc Cancer Res* **39**: 223, 1998.